ISSN 2395-1621

Subcooled Flow Boiling Heat Transfer Characteristics of Water- Al_2O_3 Nanofluid Inside a Vertical Threaded Tube

[#1]F. S. Tanekhan, [#2]B.D. Mahadik, [#3]Z. Ali, [#3]P.D.Nemade

[1]firoj.khan.1707@gmail.com
[2]mech.isbm@gmail.com

[#1,2,3,4]Mechanical Engineering Department, ISB&M School of Technology Nande, Pune

ABSTRACT

The objective of this paper is to investigate the influence of Al_2O_3 nanofluid on heat transfer coefficient during subcooled flow boiling inside a vertical copper threaded tube. The experimental data were obtained over a mass velocity range of 100 kg/m²s to 300 kg/m²s, heat flux range from 16 kW/m² to 114 kW/m² & nanoparticle mass fractions, 0.05% wt., 0.25% wt. and 0.5% wt. The results showed that the maximum heat transfer coefficient increased by 23.14% for vertical position with the pressure drop by 12.90%.

Keywords— flow boiling, internal threaded copper tube, subcooled, water-Al_2O_3.

ARTICLE INFO

Article History

Received :29th February 2016

Received in revised form :

1st March 2016

Accepted : 4th March 2016

Published online :

6th March 2016

I. INTRODUCTION

Flow boiling has long played a major role in many industrial applications due to its superior heat transfer performance such as water tube boilers, evaporators, nuclear power plants and high density electronic components. In subcooled boiling vapour bubbles generates at the heater surface while the bulk temperature of the liquid is still below the saturation temperature. Bubbles detaching from the heated surface collapse and condense in the subcooled liquid bulk. Nanofluid is a homogeneous mixture of a nanoparticles and a base fluid [1]. Also the use of augmentative techniques, either active or passive, to increase heat transfer coefficient has been studied so many times. As an example of conducted researchers, Akhvan bahabadi et al. [2] experimentally investigated evaporation heat transfer of R-134a inside a microfin tube for seven different tube inclinations ranging from -90^0 to $+90^0$. Results showed that at low vapour qualities the highest heat transfer coefficient was attained at $+90^0$ & at higher vapour qualities the highest heat transfer coefficient when tube is horizontal or was inclined at -30^0. The vertical tube with inclination angle of 90^0 had the lowest heat transfer coefficient for entire range of vapour quality. Bin sun et al. [3] experimentally studied the flow boiling heat transfer characteristics of four nanorefrigerants in an internal threaded tube. They found that maximum heat transfer coefficient of four kinds of nanorefrigerants increased by 17-25% and the heat transfer coefficient increased by 3-20%. One of the passive techniques to enhance heat transfer coefficient is the applications of internally threaded tube. Internally threaded tube can increase heat transfer through creating turbulence and limiting the growth of thermal boundary layer by slight increase in pressure drop. Many researchers have conducted experimental studies with or without passive techniques. Also the heat transfer characteristics generally keeps changing as the flow pattern changes inside the test section in the other hand the flow regime influenced by interfacial shear stress, surface tension, buoyancy and gravitational force. Akhvan Bahabadi et al. [4] studied experimentally evaporation heat transfer of R-134a inside a corrugated tube for seven different tube inclinations ranging from -90^0 to $+90^0$. They found that for low vapour quality region heat transfer coefficient for $+90^0$ inclined tube was about 62 % more than that of -90^0 inclined tube. Also for all mass velocities, the highest heat transfer coefficient were achieved for $+90^0$.

II. EXPERIMENTAL METHODS

A. Preparation of Nanofluid

Al_2O_3 nanoparticles with 30-50 nm average diameters in distilled water as base fluid with different concentrations (0.05% wt., 0.25% wt. and 0.5% wt.) were prepared at Govt. College of Pharmacy, Karad. To prepare the nanofluid suspension, the equivalent weight of nanoparticles according to their weight was measured using digital electronic balance and gradually added to distilled water while agitated in flask. The magnetic stirrer was used to agitate the nanoparticle inside the base fluid. Suspension was then vibrated for 1 hr. in ultrasonic mixer [5].

B. Experimental Apparatus

The schematic diagram of test apparatus has been shown in fig.1. The test arrangement (shown in fig.2) consists of a pre-heater, a pump, a rotameter, a test section, and a water cooled condenser. Initially the fluid is heated in preheater at 80^0C, then that fluid flows to test section through rotameter. The liquid-vapour mixture that outflowed from test section flowed into the condenser, where it is condensed into liquid. The condensed liquid passed through circulation pump to pre- heater. The pre-heater consists of a tank with 1.5 kW capacity heater was installed in it and constant AC supply was given for preheating the fluid. The test section was heated by a flexible nichrome heater wire (of 4 kW capacity) wrapped the outside of test tube. Heat flow to heater wire was monitored with a variety AC voltage controller. The voltage and current flow was measured by analog meter to determine applied heat flux.

C. Test Section

Fig.1 Photographic view of the arrangement

Fig.2 shows photographic image of test section. The test section was made of copper tube. The specifications of test section were as follows: length of test section, 1000 mm; outside diameter, 9.52 mm; inner diameter,7.52 mm; bottom wall thickness, 0.76 mm; tooth depth, 0.24 mm; tooth apex angle, 600; helix angle, 250. The test section was heated by a flexible nichrome heater wire (4 kW capacity) wrapped around the outside of test tube and five cross sections without heater wire are reserved in order to adhere thermocouples, as shown in fig. 3. Ten K- type thermocouples are located at top and bottom sides of above five cross sections of the test tube to measure the outside tube wall temperatures. The test section was insulated with ceramic wool to reduce heat loss to the surroundings. Also two thermocouples and one pressure sensor to measure temperature and pressure of fluid are installed at inlet and outlet of test section respectively.

Fig. 2 Photographic image of test section

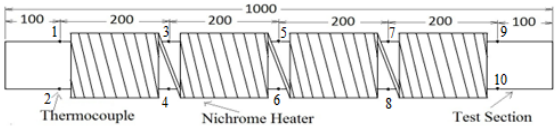

Fig. 3 The test section and layout (unit: mm)

D. Procedure

The heat transfer coefficient was calculated by using following equation,

$$\alpha = \frac{q''}{T_{wi} -} \quad (1)$$

where *q"* is the heat flux (W/m^2), *Twi* is the inner surface temperature (K), and T_f is the fluid temperature (K) calculated as follows:

$$T_f = \frac{T_{in} + T_{\ell}}{2} \quad (2)$$

where T_{in} is the inlet temperature (K) and T_{out} is the outlet temperature (K) of fluid. As the outside wall temperature of the test section was measuredat five axial locations. At each location, the temperature of the tube was measured at top and bottom positions.

$$T_{ws} = \frac{T_t +}{2} \quad (3)$$

Thus, the average outside tube wall temperature of the test section, T_{wo}, was calculated as the arithmetic mean of outside tube wall temperature at five axial locations.

$$T_{wo} = \frac{\sum_{i=1}^{5} T_i}{5} \quad (4)$$

Thermal resistance was used to measure the outside surface temperature of the tube, but the inner surface temperature was required to calculate the heat transfer coefficient. Therefore, according to Fourier's one-dimensional, radial, steady-state heat conduction equation for a hollow cylinder, based on the assumption that the heat flux is uniform inside the tube and a negligible heat loss to the surroundings, the inner surface temperature was

calculated as follows:

$$T_{wi} = T_{wo} - \frac{Q_{test} ln(d_{out}/d_i}{2\pi kl} \quad (5)$$

where, d_{out} is the outer diameter (m), d_{in} is the inner diameter (m), k is the thermal conductivity of copper (W/mK), l is the length of the test section (m), and Q_{test} is the heat flow to the test section (W) calculated from the voltage (V) and current (I) of the test section.

E. Uncertainty Analysis

The uncertainties of the experimental results are analyzed by the procedures proposed by the Kline and McClintock [4]. The method is based on careful specifications of the uncertainties in the various primary experimental measurements. The heat transfer coefficient can be obtained using the following equation (1):

$$\alpha = \frac{q''}{T_{wi} - T_f}$$

As seen from above equation, the uncertainty in the measurement of the heat transfer coefficient can be related to the errors in the measurements of voltage, current and temperatures.

$$\partial\alpha = \left\{\left[\frac{\partial\alpha}{\partial V}\delta V\right]^2 + \left[\frac{\partial\alpha}{\partial I}\delta I\right]^2 + \left[\frac{\partial\alpha}{\partial(T_{wi})}\delta(T_{wi})\right]^2 + \left[\frac{\partial\alpha}{\partial(T_f)}\delta(T_f)\right]^2\right\}^{1/2}$$

(6)

Table 1: Summary of the uncertainty analysis

Sr. No.	Parameter	Uncertainty
1	Temperature (°C)	± 0.1
2	Pressure (bar)	± 0.001
3	Water flow rate (LPH)	± 1.2
4	Voltage (V)	± 10
5	Current (A)	± 1
6	Heat transfer coefficient (W/m^2 K)	± 7.97 %

The uncertainty in determination of the flow boiling heat transfer coefficients of the present study was found to be within ± 7.97 %.The detailed results from the present uncertainty analysis for the experiments conducted here are summarized in Table 1.

III.RESULTS AND DISCUSSION

The fluid enters the test section at 80^{0}C temperature. So the degree of subcooling (ΔT=20^{0}C) is kept constant for whole experiment. In flow boiling two different regions of heat transfer has been considered: (1) convective region & (2) nucleate boiling region. The performance investigation includes the calculation of heat transfer coefficient at different heat fluxes, mass fluxes and concentration of nanoparticles.

A. Effect of Heat Flux

Experimental data are shown in terms of heat transfer coefficient vs. heat flux. In fig.4 (a) for three mass fluxes (G= 122.13 kg/m^{2}s, 203.45 kg/m^{2}s and 285.05 kg.m^{2}s), influence of heat flux on heat transfer coefficient for water is shown. With increasing heat flux, the flow boiling heat transfer coefficient increases. These increases are clearly observable in both convective and nucleate boiling zones.

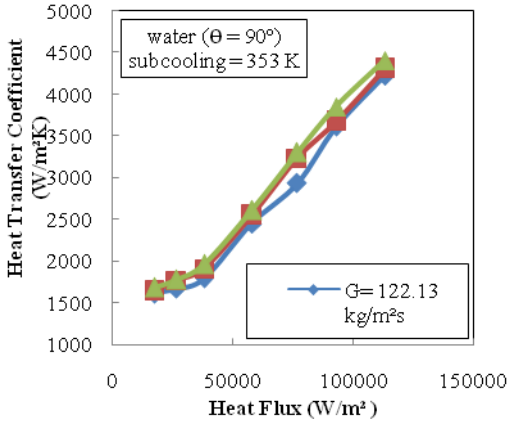

Fig. 4(a). Effect of heat flux and mass flux on heat transfer coefficient

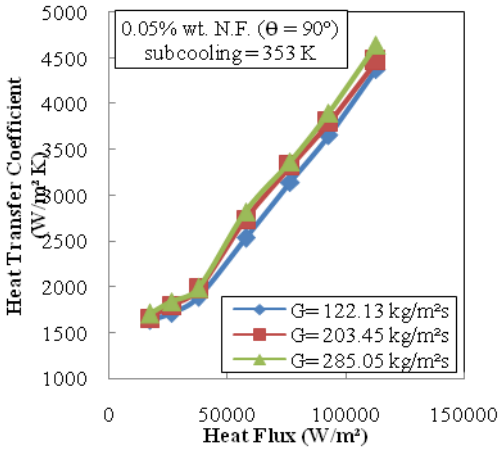

Fig. 4(b). Effect of heat flux and mass flux on heat transfer coefficient

For convective heat transfer zone increase of heat transfer coefficient with heat flux is insignificant in comparison with nucleate boiling zone. As seen in convective zone, slope of changes of flow boiling heat transfer coefficient is less than that in nucleate boiling zone. The main reason for this is, at lower heat fluxes where no bubbles generated, hence lower heat transfer coefficient. As heat flux increases, the rate of bubble generation around the heated surface increases, so that there is rigorous interaction between bubbles at heated surface which induce the locally turbulence agitations and this results in heat transfer enhancement.

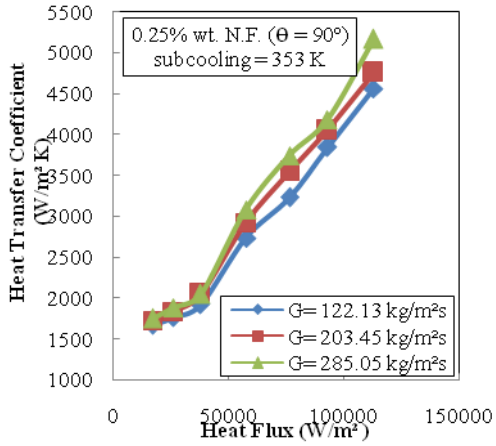

Fig.4(c). Effect of heat flux and mass flux on heat transfer coefficient

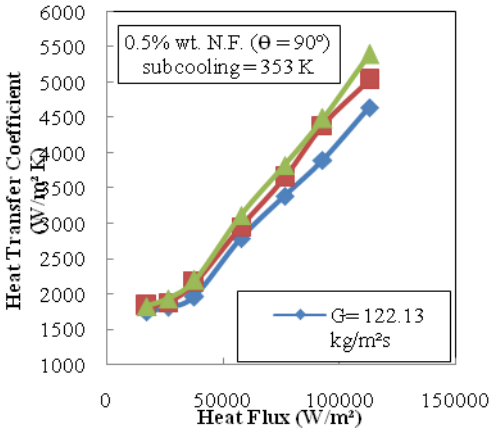

Fig.4(d). Effect of heat flux and mass flux on heat transfer coefficient

Similarly, fig.4 (b-d) shows the effect of heat flux on heat transfer coefficient for three concentrations of Nanofluid respectively.

B. Effect of Mass Flux

In above fig.4 (a-d), shows the effect of mass flux on heat transfer coefficient for vertical (θ= 90°) position of test section for water and three concentrations of nanofluid respectively. The figures shows, flow boiling heat transfer coefficient increase with increasing mass flux in both convective and nucleate boiling regions. At all the mass fluxes the increase in the heat transfer coefficient in the nucleate boiling region is considerably higher than in the convective region.

C. Effect of Nanoparticle Concentration

Fig.5 shows the effect of nanoparticle concentration on heat transfer coefficient at higher mass flux (G =285.05 kg/m^{2}s) for vertical position of test section. The obtained result shows that as the particle concentration increases, heat transfer coefficient also increases. The main reason for that is with the addition of nanoparticles, thermal conductivity of fluid increases. However, for forced convective region, slight increase of heat transfer coefficient is seen while for nucleate boiling heat transfer zone, heat transfer coefficient dramatically increases. Fig.5 shows the heat transfer coefficient enhancement of 1.49-8.67% in convective region and 5.93-23.14% in nucleate boiling region.

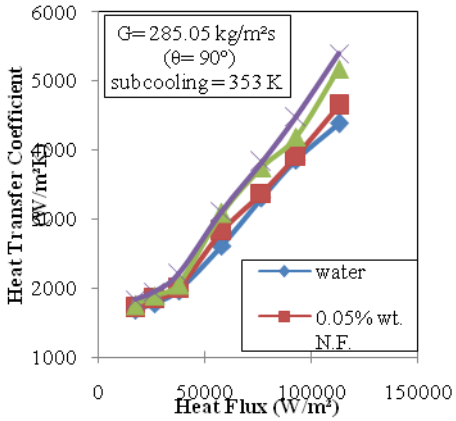

Fig.5. Effect of nanoparticle concentration on heat transfer coefficient

D. Pressure Drop

Fig.6 shows the effect of mass flux and nanoparticle concentration on pressure drop for highest heat flux (q"=113.095 kW/m^2) and vertical position (Θ = 90^0) of test section. From fig.6, it can be seen that as the mass flux increases the pressure drop also increases, also as the concentration of nanoparticle increases the pressure drop increases. The reason is that as the nanoparticle concentration in water increases the viscosity of nanofluid increases. For vertical position (Θ= 90°) of test section at mass flux 285.05 kg/m^{2}s and 0.5% wt. Al_2O_3 nanofluid, the pressure drop is 12.90 % more than the pressure drop for water.

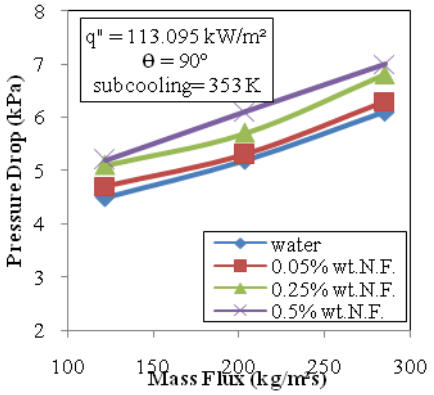

Fig.6. Effect of nanoparticle concentration on pressure drop

IV. CONCLUSION

Heat transfer coefficient increases with the increase in heat flux, mass flux and concentration of nanoparticles. The increase in heat transfer coefficient in nucleate boiling region is much more compared to the increase in heat transfer coefficient in convective region. In forced convective region the maximum heat transfer enhancement is 8.675% enhancement for 0.5 % wt. concentration Al_2O_3

nanofluid at mass flux 285.05 kg/m^{2}s. In nucleate boiling region the maximum heat transfer enhancement is 23.14% for 0.5 % wt. concentration Al_2O_3 nanofluid at mass flux 285.05 kg/m^{2}s. The pressure drop increases as the concentration of nanoparticle increases in base fluid. The increase in pressure drop is about 12.90% for vertical position (θ=90°) of test section for 0.5% wt. Al_2O_3 nanofluid at mass flux of 285.05 kg/m^{2}s.

REFERENCES

[1] Choi SUS, 1995, "Enhancing thermal conductivity of fluids with nanoparticles", ASME FED, 231, pp.99–105.

[2] Akhavan-Behabadi M.A., Mohseni S. G., Razavinasab S.M., 2010, "Evaporation heat transfer of R-134a inside a microfin tube with different tube inclinations", Experimental Thermal and Fluid Science, 35, pp. 996–1001C. Y. Lin, M. Wu, J. A. Bloom, I. J. Cox, and M. Miller, "Rotation, scale, and translation resilient public watermarking for images," IEEE Trans. Image Process., vol. 10, no. 5, pp. 767-782, May 2001.

[3] Sun B., Yang D., 2013, "Experimental study on the heat transfer characteristics of nanorefrigerants in an internal thread copper tube", International Journal of Heat and Mass Transfer, 64, pp. 559–566.

[4] Akhavan-Behabadi M. A., M. Esmailpour, 2014, "Experimental study of evaporation heat transfer of R-134a inside a corrugated tube with different tube inclinations", International Communications in Heat and Mass Transfer, 55, pp. 8–14.

[5] Heyhat M.M., Kowsary F., Rashidi A.M., Momenpour M.H., Amrollahi A.,2013, "Experimental investigation of laminar convective heat transfer and pressure drop of water-based Al_2O_3 nanofluids in fully developed flow regime", Experimental Thermal and Fluid Science, 44, pp. 483–489.

[6] Copetti J. B., Macagnan M. H., De Souza D., Césaro Oliveski R. De, 2003, "Experimental study on thermal and hydraulic behavior of micro-fin tubes in single phase", 17th International Congress of Mechanical Engineering, November, pp. 10-14, São Paulo, SP.

[7] Cavallini A., Del Col D., Doretti L., Longo G.A., Rossetto L., 2000, "Heat transfer and pressure drop during condensation of refrigeration inside horizontal enhanced tubes", International Journal of Refrigeration, 23, pp. 4–25.

